FPCM-9 (2008)
The 9th International Conference on Flow Processes in Composite Materials
Montréal (Québec), Canada
8 ~ 10 July 2008

NUMERICAL PREDICTION OF MESO-SCALE VOIDS IN LIQUID COMPOSITE MOULDING AND EXPERIMENTAL VALIDATION INCLUDING VARIABILITY STUDY

J.S.U. Schell [1], M. Deleglise [2], C. Binetruy [2, 3], P. Krawczak [2] and P. Ermanni [1]

[1] *ETH Zurich, Centre of Structure Technologies, Leonhardstr. 27, CH-8092 Zurich, Switzerland, Email: permanni@ethz.ch*
[2] *Ecole des Mines de Douai, Technology of Polymers and Composites and Mechanical Engineering Department, 941 rue Bourseul, BP 10838, 59508 Douai Cedex,France*
[3] *Corresponding author's Email: binetruy@ensm-douai.fr*

SUMMARY: In Liquid Composite Moulding (LCM) processes the pressure gradients can vary between very high and very low gradients depending on the distance to the injection gate and the part size. Meso-scale voids, which dramatically reduce the composite part quality, are created at very low pressure gradients. In contrast, high pressure gradients favour the micro-void creation. In this contribution, a numerical method is presented to predict the meso-scale creation. The prediction of the meso-scale voids is validated by measuring the void content of produced composite parts with micro-computed tomography (μ-CT). Additionally, the influence of the fibre volume content on the meso-and micro-scale-void content is studied.

KEYWORDS: meso-scale voids, micro-voids, mesostructure, Liquid Composite Moulding (LCM), micro-computed tomography (μ-CT), fibre bundle

INTRODUCTION

Liquid Composite Moulding (LCM) processes are suited to manufacture large and complex composite parts. Resin flow at the macroscopic level can have a very predictable shape. However, at the meso-scale level and because of the woven structure of the fabric, a secondary flow takes place inside the fiber bundles. The dual scale of porous media created by the large difference between intra- and inter- bundle permeability is the reason for void generation. For instance, for large parts manufactured at low injection pressure, resin velocity variations can be important. As resin velocity is a major parameter in the process of void generation, the nature and size of voids change with the velocity inside the part: at high resin velocities, micro-voids are created inside the fibre bundles and at low velocities, as illustrated in Fig. 1, meso-scale voids are created between the bundles [1]. The prediction of voids requires a simulation tool which takes

into account both void generation mechanisms. Gourichon et al. [2] developed a simulation code based on LIMS software to predict micro-void generation, their evolution and their elimination. In this contribution, following the same approach, the simulation of meso-scale void creation and evolution is developed in order to complete the prediction possibilities.

MATHEMATICAL MODEL OF MESO-SCALE-VOID GENERATION

Meso-scale-voids are created at very low pressure gradients during the impregnation of a preform. At the flow front, the intra-bundle flow is driven by the capillary pressure P_{cap}:

$$P_{cap} = \frac{2\gamma \cos\theta}{r} \tag{1}$$

where γ is the resin surface tension, θ the contact angle and r the capillary radius. In this case, the velocity in the longitudinally oriented fibre bundles, u_b, is faster than the velocities in the inter-bundles areas, uib, for definition of the velocities see Fig. 1. The velocity u_b is derived from Darcy's law:

$$u_b = \frac{K_{long}}{\mu} \frac{\Delta p + P_{cap}}{l_{warp}} \tag{2}$$

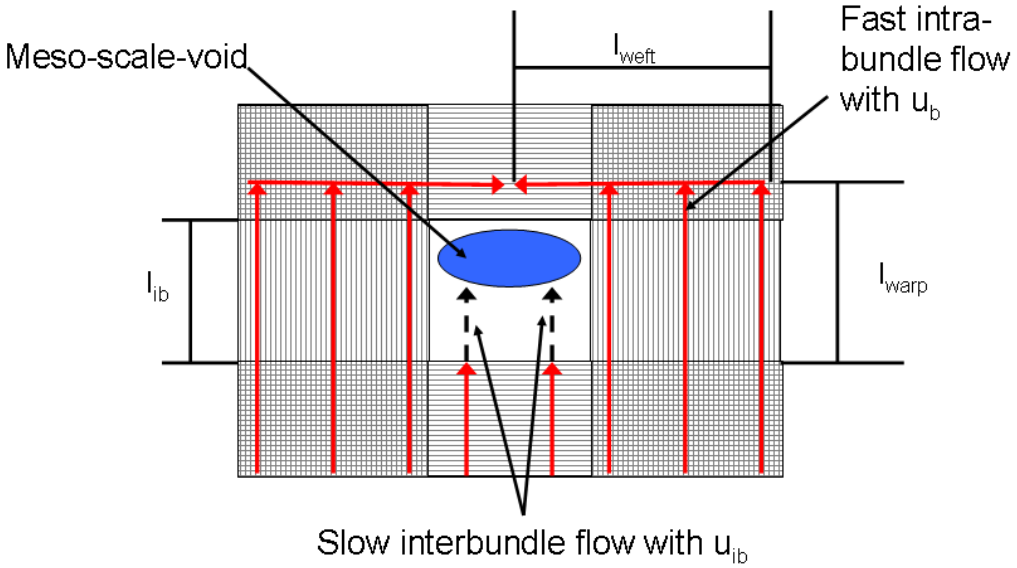

Fig. 1 Flow path for meso-scale void creation.

where K_{long} is the longitudinal fibre bundle permeability, μ the resin viscosity, Δp is the fluid pressure loss over the flow distance in the bundles l_{warp} as defined in Fig. 1. The velocity u_{ib} is derived from Darcy's law:

$$u_{ib} = \frac{K_{sat}}{\mu}\frac{dp}{dl} \tag{3}$$

where K_{sat} is the saturated permeability of the fabric and dp/dl is the fluid pressure gradient over a length dl. Air is entrapped if the resin flows faster inside the bundles than between them (Fig. 1). A meso-scale void is created.

NUMERICAL APPROACH

For the prediction of the meso- and micro-scale-void creation, the flows in the inter-bundle regions and inside the bundles have to be modelled and implemented in a simulation tool. The simulation package LIMS offers this possibility [3]. For the prediction of fibre bundle saturation, 1D element (composed of one bar element and two nodes) are added to the 2D elements of the FE-mesh as shown in Fig. 2. Those 1D elements represent the transverse bundles that are likely to entrap air creating micro-voids. They act as sinks, and their filling state represents saturation in the bundles. The 2D elements represent the inter-bundle spaces and the longitudinal bundles. As a result, micro-pores are generated in the 1D element whereas meso-scale-pores are generated in the 2D elements [2].

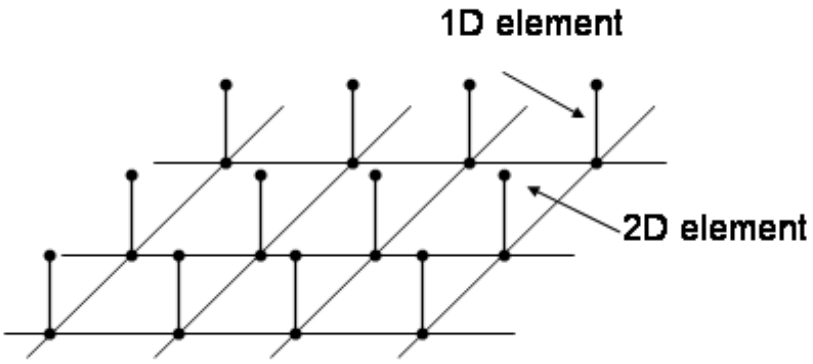

Fig. 2 Finite element mesh with 1D elements.

As 1D elements represent the transversal fibre bundles, properties assigned to the 1D elements are the bundle transversal permeability, the bundle dimensions (length and cross-section) and fibre volume content in the bundles v_{fb}. The permeability of the 2D elements is the macroscopic saturated permeability of the fabric.

For the prediction of the mesoscale-void generation the times of the intra-bundle flow and of the inter-bundle flow is compared. The time, t_{warp}, necessary to impregnate the distance l_{warp} in the warp bundle is calculated with:

$$t_{warp} = \frac{\mu l^2_{warp}\phi_b}{K_{long}(\Delta p + P_{cap})} \tag{4}$$

derived from Darcy's law Eq. (2), with $\Phi_b = 1\text{-}v_{fb}$ and Δp_i the imposed pressure difference at the node i considered. The flow inside the weft bundle is driven by the capillary pressure P_{cap}. The time t_{weft} necessary to impregnate the distance l_{weft} is expressed as follows:

$$t_{weft} = \frac{\mu l^2_{weft} \phi_b}{K_{long} P_{cap}} \tag{5}$$

The time to flow through the inter-bundle region with the length l_{ib} in the 2D element is t_{ib}, calculated by Darcy's law at the node i:

$$t_{ib} = \frac{\mu l^2_{ib} \phi}{K_{sat} \Delta p_i} \tag{6}$$

where $\Phi = 1\text{-}v_b$, where v_b is the bundle volume content. These time calculations are done at each calculation step n. If t_{ib} is longer than t_{tot} defined by $t_{tot} = t_{weft} + t_{warp}$ then air is entrapped in the 2D element. The air content is calculated based on the filled length and the fibre volume content. Compression of the air bubbles due to increasing resin pressure is taken into account according to the ideal gas law.

EXPERIMENTAL

The fabric is a balanced roving fabric, from Interglas, having an arial density of 600 g/m2. Its saturated permeability (K_{sat}) measured using 1D flow experiments was found to be 5.6 10^{-11} m^2 for a 53% fibre volume fraction configuration. The transversal and longitudinal permeabilities K_{trans} and K_{long} were measured with a special experimental setup presented in [4]. The resin system is epoxy resin L 1100 and hardener EPH294 from Hexion. This resin system has a pot life of 500 min and a viscosity of 0.29 Pa.s at 25°C. The resin is assumed to have a perfect wettability so its contact angle is set to 0°. Table 1 lists the values of the inputs for the simulation.

Table 1 Input data with their standard deviations

Variable	Value	Standard deviation%
K_{sat} (m^2)	5.6 10^{-11}	10
K_{trans} (m^2)	2.6 10^{-13}	16
K_{long} (m^2)	6.1 10^{-12}	38
v_{fb} (%)	64	10
v_b (%)	83	10
l_{ib} (m)	0.004	9
l_{warp} (m)	0.0041	9
l_{weft} (m)	0.004	9
h_{weft} (m)	0.0002	8
r (m)	2.5 10^{-6}	35
μ (Pa s)	0.29	
γ (N/m)	0.024	
θ	0°	

Samples for the experimental validation were produced using an injectomat cp-IS from Fresenius which enables an injection at a low constant flow rate. The dimensions of the mould are 0.05 x

0.01 x 0.225 m^3. The resin was injected at a flow rate of 1.39 x 10^{-10} m^3/s at room-temperature. After curing, the part was removed from the mould and samples with a width of around 0.008 m were cut out from the vent region. 5 composite parts were manufactured for this study. This very low flow rate was chosen to be in the capillary driven flow regime close to the process window of minimal void content. To determine the meso-scale void content, the samples were scanned in a micro computed tomography scanner described in [5].

RESULTS AND DISCUSSION

The simulation using the LIMS software was run with the input data presented in Table 1 corresponding to the experimental conditions and a flow rate of 1.39x10^{-10} m^{-3}/s at the injection line. As the simulation is carried out at low pressure gradients, the bundles are impregnated prior to the inter-bundle regions. The numerical calculation predicts a meso-scale-void content of 8%. The investigation of the composite parts with the μ-CT gives an average air content of 5.5 ± 0.6%.

The simulation is refined by including into the simulation the standard deviations of the measured input values concerning the fabric like the permeabilities and the bundle distances (see Table 1). The values characterising the resin remain constant. Two simulations are carried out at both ends of the 68% confidence interval of the input values. Two simulations are thus conducted, sim+ at the upper end and sim- at the lower end. The reference values are the saturated permeability K_{sat} and the fibre volume content in the bundles v_{fb}. The other parameters vary for consistency. For example, if K_{sat} is increased in sim+, bundles are considered more packed, thus the tow permeabilities K_{long} and K_{trans} decrease. Simulation sim+ predicts a meso-scale-void content of 4%, and sim- a content of 11%. The reduction of the meso-scale-void content in sim+ compared to the 8% in the simulation without any confidence interval is a result of the decreased longitudinal fibre permeability and increased saturated permeability.

The influence of the fibre volume content in the bundles on the void creation is studied in a pure numerical study. The fibre volume content in the bundles v_{fb} is increased from 68% to 80%. The capillary radius r, the transversal and longitudinal permeability K_{long} and K_{trans} are taken as a function of v_{fb} according to Gebart's model [6]. With increasing v_{fb} the meso-scale-void content decreases and the micro-scale-void content increases. This is a result of the decreasing bundle permeabilities K_{trans} and K_{long} with increasing v_{fb}. Decreasing K_{trans} with decreasing r hinders the bundle impregnation, resulting in an increase of the micro-scale void content. The decrease of K_{long} prolongs the intra-bundle fill time, resulting in a lower meso-scale void content.

CONCLUSIONS

The presented method enables the prediction of the meso-scale and the micro-scale-void content in one simulation. As the simulation is based on experimentally determined inputs, the variability of these values has to be included in the simulation. This is realised in the refined simulation. The experimentally determined void content is in the enlarged prediction of the refined simulation. The parametric study of the fibre volume content in the bundles showed its influence on microscopic and mesoscopic scale void contents.

ACKNOWLEDGEMENTS

The authors gratefully acknowledge support by the Swiss National Science Foundation under Contract No. 200020-109109/1. The μ-CT measurements were performed by courtesy of the Institute for Biomedical Engineering, University and ETH Zurich.

REFERENCES

1. Kang, M. K., Lee, W. I., Hahn, H. T., "Formation of Micro-voids during Resin Transfer Molding Process", *Composites Science and Technology*, Vol. 60, 2000, pages 2427-2434.

2. Gourichon, B., Binetruy, C., Krawczak, P., "A New Numerical Procedure to Predict Dynamic Void Content in Liquid Composite Molding", *Composites: Part A: Applied Science and Manufacturing*, Vol. 37, Issue 11, 2006, pages1961-1969.

3. Simacek P., Advani S.G., "A Numerical Method to Predict Fiber Tow Saturation during Liquid Composite Molding", *Composites Science and Technology*, Vol. 63, 2003, pages 1725-1736.

4. Schell J., Siegrist M., Ermanni P., "Experimental Determination of the Transversal and Longitudinal Fibre Bundle Permeability", *Applied Composite Materials*, Vol. 14, 2007, pages 117–128.

5. Schell J., Renggli M, van Lenthe GH, Müller R, Ermanni P., "Micro-Computed Tomography Determination of Glass Fibre Reinforced Polymer Meso-Structure", *Composite Science and Technology*, Vol. 66, 2006, pages 2016–2022.

6. Gebart B., "Permeability of Unidirectional Reinforcements for RTM", *J Composite Materials*, Vol. 26, 1992, pages 1100–1133.